DALTON
FULL PAPER

Synthesis, structure and redox behaviour of facial $[Re^{III}L(PPh_3)Cl_3]$ and its stereoretentive conversion to $[Re^{IV}L'(PPh_3)Cl_3]$ *via* metal promoted aldimine ⟶ amide oxidation (L = pyridine-2-aldimine; L′ = pyridine-2-carboxamide)

Sibaprasad Bhattacharyya, Sangeeta Banerjee, Bimal Kumar Dirghangi, Mahua Menon and Animesh Chakravorty *

Department of Inorganic Chemistry, Indian Association for the Cultivation of Science, Calcutta 700 032, India

Received 11th August 1998, Accepted 29th October 1998

The reaction of *mer*-$[Re^{III}L(OPPh_3)Cl_3]$ **2** with PPh_3 in benzene has afforded bluish violet *fac*-$[Re^{III}L(PPh_3)Cl_3]$ **1**, where L is the Schiff base of pyridine-2-carbaldehyde and the substituted aniline *p*-$XC_6H_4NH_2$ (X = H, Me, OMe or Cl). Geometrical preferences are rationalized in terms of the electronic nature of the ligands $OPPh_3$ (σ- and π-donor), PPh_3 (σ-donor and π-acceptor) and L (σ-donor and π-acceptor). The cyclic voltammetric $E_{1/2}$ values of **1** lie near 0.6 V (Re^{IV}–Re^{III}) and −0.6 V (Re^{III}–Re^{II}). Electrooxidation of **1** at 1.0 V *vs.* SCE in wet acetonitrile affords yellow *fac*-$[Re^{IV}L'(PPh_3)Cl_3]$ **3** which is also obtainable *via* oxidation by dilute nitric acid (L′ is a monoanionic pyridine-2-carboxamide). Complex **3** displays Re^{IV}–Re^{III} and Re^{V}–Re^{IV} couples near −0.2 V and 1.4 V respectively reflecting superior stabilization of the rhenium(IV) state by the amide ligand. The X-ray structures of two representative complexes of type **1** and **3** have revealed the presence of severely distorted and facially configured $RePN_2Cl_3$ coordination spheres. The average Re–Cl distance is lower by 0.06 Å in **3** due to contraction of the metal radius upon oxidation. The Re–P length is however larger by 0.1 Å in **3** signifying a weakening of Re–P back-bonding.

The rhenium chemistry of Schiff bases of pyridine-2-carbaldehyde is under scrutiny in this laboratory. Facile oxygen-atom-transfer, metal-mediated ligand oxidation and stabilization of unusual rhenium moieties are among the notable features that have so far been documented.[1–6] In this work we disclose a spontaneous geometrical transformation associated with ligand substitution. The reaction has afforded a family of pyridine-2-aldimine chelates of trivalent rhenium incorporating phosphine coordination. The species are redox active and undergo facile aldimine ⟶ amide oxidation. The structure and properties of the present complexes and their oxidized derivatives are described.

Results and discussion

Synthesis of *fac*-$[ReL(PPh_3)Cl_3]$ 1

Four pyridine-2-aldimine ligands (L^1–L^4; general abbreviation is L), differing in the X substituent have been utilized. The complexes have facial geometry (see below) and are formed upon reacting the meridional phosphine oxide complexes of type $[ReL(OPPh_3)Cl_3]$ **2**,[1–3] with PPh_3, in boiling benzene, equation (1). The reaction of *mer*-$[ReOCl_3(PPh_3)_2]$ with L also furnishes **1**, equation (2), but in poorer yield.

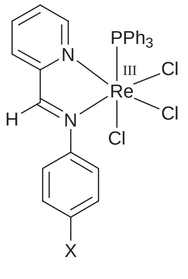

1a $[ReL^1(PPh_3)Cl_3]$ (X = H)
1b $[ReL^2(PPh_3)Cl_3]$ (X = Me)
1c $[ReL^3(PPh_3)Cl_3]$ (X = OMe)
1d $[ReL^4(PPh_3)Cl_3]$ (X = Cl)

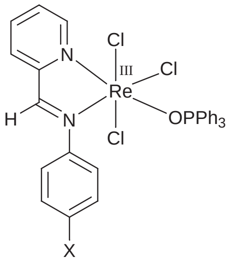

2 $[ReL(OPPh_3)Cl_3]$

$$mer\text{-}[ReL(OPPh_3)Cl_3] + PPh_3 \longrightarrow fac\text{-}[ReL(PPh_3)Cl_3] + OPPh_3 \quad (1)$$

$$mer\text{-}[ReOCl_3(PPh_3)_2] + L \longrightarrow fac\text{-}[ReL(PPh_3)Cl_3] + OPPh_3 \quad (2)$$

Selected spectral and magnetic characterization data for the complexes are listed in Tables 1 and 2. The magnetic moments (≈2 μ_B, Table 1) are lower than the spin-only value for the $t_{2g}{}^4$ (assuming idealised octahedral geometry) configuration which is not unusual for trivalent rhenium.[7] The paramagnetically shifted ^1H NMR signals of **1** have been assigned (Table 2) on the basis of signal intensity, spin–spin structure and previous work.[8–10] A selected portion of the ^1H NMR spectrum of **1b** is displayed in Fig. 1.

Structure

The X-ray structure of *fac*-$[ReL^1(PPh_3)Cl_3]$ **1a** has been determined. A molecular view is shown in Fig. 2 and selected bond parameters are listed in Table 3. The aldimine and phosphine ligands are facially disposed and so are the chloride ligands, forming a severely distorted octahedral $RePN_2Cl_3$ coordination sphere. The chelate ring along with the pyridine ring and Cl(2), Cl(3) atoms constitute a good plane (mean deviation 0.05 Å) to which the pendent phenyl ring makes a dihedral angle of 50.1°.

The X-ray structures of a few Re^{III}–PPh_3 complexes are known.[8,11,12] Only one of these has the $ReCl_3$ moiety but in a meridional configuration.[8] To the best of our knowledge **1a** is the first structurally characterized PPh_3 complex having facial $ReCl_3$ disposition. The Re–P distance, 2.463(2) Å in **1a** is normal.[8,12]

Table 1 Electronic spectral,[a] IR[b] and magnetic moment data at 298 K

Compound	UV/VIS λ_{max}/nm (ε/dm^{-3} mol^{-1} cm^{-1})	IR ν/cm^{-1}	μ_{eff}/μ_B
1a [ReL^1(PPh$_3$)Cl$_3$]	1575(260), 665(2085), 525(3250), 405(2985), 300[c](10230)	320, 335, 510, 700, 1600	2.02
1b [ReL^2(PPh$_3$)Cl$_3$]	1575(205), 665(2345), 525(4320), 400(2840), 300[c](10865)	315, 335, 510, 700, 1590	2.10
1c [ReL^3(PPh$_3$)Cl$_3$]	1560(370), 670(2530), 525(3820), 400(2910), 300[c](10430)	330, 510, 710, 1595	2.15
1d [ReL^4(PPh$_3$)Cl$_3$]	1565(350), 670(2460), 525(3360), 410(2890), 310[c](10000)	320, 500, 700, 1585	2.05
3a [ReL$^{1'}$(PPh$_3$)Cl$_3$]	430(3775), 300(7350)	320, 330, 500, 710, 1600, 1640	3.32
3b [ReL$^{2'}$(PPh$_3$)Cl$_3$]	440(2900), 300(7310)	315, 330, 510, 700, 1610, 1640	3.41
3c [ReL$^{3'}$(PPh$_3$)Cl$_3$]	440(2860), 295(6940)	335, 510, 700, 1605, 1630	3.45
3d [ReL$^{4'}$(PPh$_3$)Cl$_3$]	440(3010), 295(7185)	320, 330, 500, 700, 1610, 1630	3.38

[a] In dichloromethane. [b] In KBr disc; ν(R–Cl) 310–335, ν(C=N) 1590–1600, ν(PPh$_3$) 510, 700, ν(C=O) 1600–1640 cm^{-1}. [c] Shoulder.

Table 2 ^{1}H NMR data in CDCl$_3$

	δ		
	1a	**1b**	**1d**
o-H(d)	13.80	13.70	13.50
m-H(t)	8.96	8.96	8.90
p-H(t)	8.73	8.74	8.76
1-H(d)	25.70	24.80	26.70
2-H(t)	−11.40	−11.00	−11.90
3-H(t)	5.23	5.27	5.29
4-H(d)	5.00	4.60	4.70
6-H(s)	−46.00	−47.60	−43.60
8,12-H(d)	21.35	20.9	21.00
9,11-H(d)	11.85(t)	11.44	11.62
10-H(t)	7.70	—	—
CH$_3$(s)	—	3.64	—

Tetramethylsilane was used as internal standard; s = singlet, d = doublet, t = triplet.

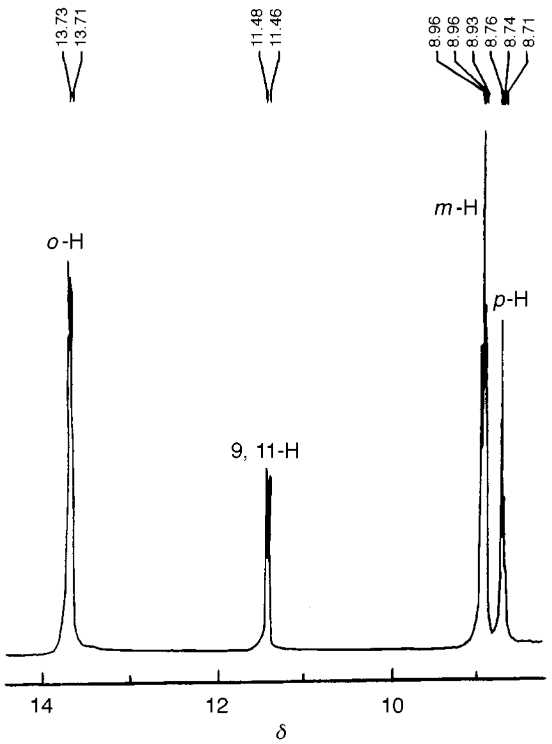

Fig. 1 A part of the proton NMR spectrum of *fac*-[ReL^2(PPh$_3$)Cl$_3$] **1b** in CDCl$_3$ solution; *o*-H, *m*-H and *p*-H refer respectively to *ortho*, *meta* and *para* protons of PPh$_3$.

Geometrical preference

The striking geometrical difference between **1** and **2** is believed to be of electronic origin. In **1**, PPh$_3$ is a π-accepting ligand, the acceptor orbital being a mixture of 3d$_\pi$ and P–C σ* components.[13] The L ligand is also π-accepting due to the α-diimine function (–N=C–C=N–).[2,14] Trivalent rhenium is prone to back-bonding.[15] Assuming idealised octahedral geometry this bonding has $t_{2g}(Re) \longrightarrow \pi(P)$ and $t_{2g}(Re) \longrightarrow \pi^*(L)$ components in **1**. Back-bonding is maximized when the acceptor ligands are facially disposed so that competition between ligands for identical metal orbitals is minimal.

Table 3 Selected bond lengths (Å) and angles (°) for complexes **1a** and **3d**

	1a	**3d**
Re–N(1)	2.103(5)	2.123(7)
Re–N(2)	2.083(5)	2.061(7)
Re–Cl(1)	2.407(2)	2.331(3)
Re–Cl(2)	2.350(2)	2.300(3)
Re–Cl(3)	2.379(2)	2.345(3)
Re–P	2.463(2)	2.549(3)
N(1)–C(5)	1.371(8)	1.336(12)
N(2)–C(6)	1.309(8)	1.349(12)
C(5)–C(6)	1.408(9)	1.524(13)
O(1)–C(6)	—	1.217(11)
N(2)–Re–N(1)	75.9(2)	78.2(3)
N(2)–Re–Cl(2)	99.5(2)	95.1(2)
N(1)–Re–Cl(2)	174.1(2)	173.2(2)
N(2)–Re–Cl(1)	87.0(2)	90.2(2)
N(2)–Re–Cl(3)	167.0(2)	170.1(2)
N(1)–Re–Cl(1)	86.3(2)	86.0(2)
N(1)–Re–Cl(3)	91.3(2)	92.0(2)
Cl(2)–Re–Cl(3)	93.18(7)	94.77(11)
Cl(2)–Re–Cl(1)	89.74(7)	94.42(11)
Cl(3)–Re–Cl(1)	90.46(8)	90.53(11)
N(2)–Re–P	93.7(2)	93.7(2)
N(1)–Re–P	97.0(2)	90.7(2)
Cl(2)–Re–P	86.97(7)	89.37(10)
Cl(1)–Re–P	176.70(6)	174.29(9)
Cl(3)–Re–P	89.55(7)	84.89(10)
C(5)–N(1)–Re	115.8(4)	114.5(6)
C(6)–N(2)–Re	116.6(5)	118.2(6)
N(1)–C(5)–C(6)	113.5(6)	116.3(8)
O(1)–C(6)–N(2)	—	127.1(9)

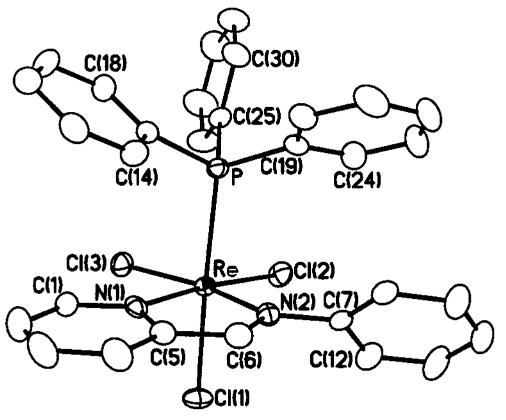

Fig. 2 A view of [ReL^1(PPh$_3$)Cl$_3$] **1a**; the atoms are represented by their 30% thermal probability ellipsoids.

Table 4 Cyclic voltammetric formal potential[a] at 298 K

Compound	$E_{\frac{1}{2}}$/V (ΔE_p/mV)
1a	−0.60(100), 0.65(80)
1b	−0.61(100), 0.62(80)
1c	−0.64(100), 0.58(80)
1d	−0.59(100), 0.68(80)
3a	−0.10(80), 1.28(80)
3b	−0.15(80), 1.19(80)
3c	−0.18(80), 1.10(80)
3d	−0.06(80), 1.35(80)

[a] Solvent, dichloromethane; scan rate, 50 mV s^{-1}; $E_{\frac{1}{2}} = 1/2\ (E_{pa} + E_{pc})$ where E_{pa} and E_{pc} are anodic and cathodic peak potentials respectively; $\Delta E_p = E_{pc} - E_{pa}$. Reference electrode, SCE. The concerned couples are **1**–$\mathbf{1}^-$ (Re^{III}–Re^{II}), $\mathbf{1}^+$–**1** (Re^{IV}–Re^{III}), **3**–$\mathbf{3}^-$ (Re^{IV}–Re^{III}), $\mathbf{3}^+$–**3** (Re^{V}–Re^{IV}).

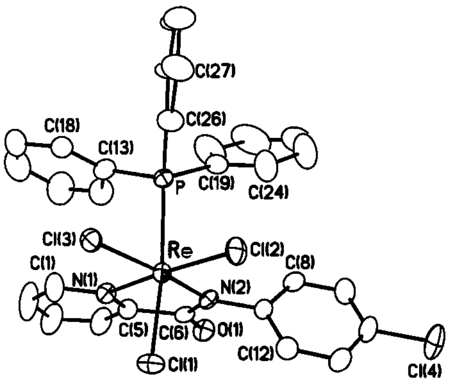

Fig. 3 A view of $[ReL^{4'}(PPh_3)Cl_3]$ **3d**; the atoms are represented by their 30% thermal probability ellipsoids.

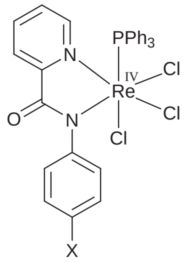

3a $[ReL^{1'}(PPh_3)Cl_3]$ (X = H)
3b $[ReL^{2'}(PPh_3)Cl_3]$ (X = Me)
3c $[ReL^{3'}(PPh_3)Cl_3]$ (X = OMe)
3d $[ReL^{4'}(PPh_3)Cl_3]$ (X = Cl)

The meridional geometry is expected to be favoured by steric as well as electrostatic factors. In the case of **1** these advantages are more than offset by the superior back-bonding of the facial configuration. This does not apply to $[ReL(OPPh_3)Cl_3]$ since $OPPh_3$ is purely a donor in both σ and π senses. Hence its geometry is logically meridional. It is instructive to compare the metal–ligand bond distances of **1a** with those of *mer*-$[ReL^2(OPPh_3)Cl_3]$.[2] The average Re–Cl length of two complexes are nearly equal (2.37–2.38 Å). However the Re–N lengths in **1a** are *ca.* 0.06 Å longer than those in the phosphine oxide complex where L^2 alone is available for back-bonding $[t_{2g}(Re) \longrightarrow \pi^*(L^2)]$.

The geometrical selectivity in **1** and **2** is strong and exclusive. In no case have isomers been observed. It is noteworthy that $[ReL(O)Cl_3]$[3] and $[ReL(NAr)Cl_3]$[5,6] are meridional, the O and NAr ligands being pure donors like $OPPh_3$. Upon reacting **1** with aromatic amines ($ArNH_2$) in benzene solution in air, facile and quantitative transformation to *mer*-$[ReL(NAr)Cl_3]$ occurs. This reaction (*fac* ⟶ *mer*) represents a reversal of the geometrical change (*mer* ⟶ *fac*) characterizing the reaction of equation (1).

Metal redox: formation of $[ReL'(PPh_3)Cl_3]$ 3

The *fac*-$[ReL(PPh_3)Cl_3]$ complexes are electroactive in dichloromethane solution displaying two quasi-reversible one-electron responses in the range −0.5 to 0.7 V *vs.* SCE. Reduction potential data are listed in Table 4. The responses are assigned to the Re^{IV}–Re^{III} ($E_{1/2} \approx 0.6$ V) and Re^{III}–Re^{II} ($E_{1/2} \approx -0.6$ V) couples. In **2** the Re^{IV}–Re^{III} couple occurs at *ca.* 0.3 V.[3] Thus the trivalent state of rhenium is more difficult to oxidize in **1** than in **2**. This is consistent with the presence of phosphine back-bonding in **1**.

The red oxidized complex $[Re^{IV}L(PPh_3)Cl_3]^+$ $\mathbf{1}^+$ can be generated in solution by coulometric oxidation of **1** in dry acetonitrile at 1.0 V. It reacts spontaneously with added water affording the amide complex *fac*-$[Re^{IV}L'(PPh_3)Cl_3]$ **3**, equation (3). The facial geometry is conserved in the conversion of

$$3\,[Re^{IV}L(PPh_3)Cl_3]^+ + H_2O \longrightarrow \\ fac\text{-}[Re^{IV}L'(PPh_3)Cl_3] + 2\,fac\text{-}[Re^{III}L(PPh_3)Cl_3] + 3H^+ \quad (3)$$

1 ⟶ **3**, *vide infra*. When coulometry is performed in moist acetonitrile the regenerated *fac*-$[Re^{III}L(PPh_3)Cl_3]$ complex, equation (3), is reoxidized and in this manner the whole of **1** is finally converted to **3**. The total coulomb count at full conversion corresponds to the transfer of three electrons. From the electrolytic solution **3** can be isolated in excellent yields.

These findings encouraged us to explore the chemical oxidation of **1** to **3**. Aqueous nitric acid and hydrogen peroxide were indeed found to be very effective. The most convenient synthesis of **3** is based on aqueous nitric acid oxidation of **1** in acetonitrile solution.

Aldimine ⟶ amide conversion in oxidizing aqueous environments has previously been observed[2] in the cases of **2** and *mer*-$[ReL(NAr)Cl_3]$.[5,6] Rate studies on **2**[3] and on a ruthenium system[16] have demonstrated that the reaction proceeds by the addition of a molecule of water to the aldimine function polarized by metal oxidation. In the present case the oxidized metal is rhenium(IV) as in $\mathbf{1}^+$. Rapid oxidation of the corresponding water adduct **4** *via* induced transfer to two electrons[17] associated with proton dissociation, can afford **3**.

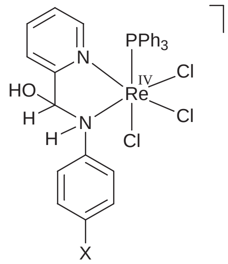

4

Spectral and magnetic data for *fac*-$[Re^{IV}L'(PPh_3)Cl_3]$ **3** are listed in Table 1. The magnetic moments are lower[3] than the $t_{2g}{}^3$ (assuming idealised octahedral geometry) spin-only value. Two strong amide stretches occur in the range 1600–1640 cm^{-1}. In dichloromethane solution **3** displays two quasi-reversible cyclic voltammetric responses in the range of −0.2 to 1.4 V corresponding to the couples Re^{IV}–Re^{III} ($E_{1/2} \approx -0.2$ V) and Re^{V}–Re^{IV} ($E_{1/2} \approx 1.4$ V) (Table 4). Thus the Re^{IV}–Re^{III} couple moves to lower potential by ~700 mV in going from **1** to **3** reflecting the ease of Re^{III}–Re^{IV} oxidation upon amide binding.

The facial geometry of **3** has been proven by structure determination of $[ReL^{4'}(PPh_3)Cl_3]$ **3d** (Fig. 3, Table 3). As in **1a** the chelate ring, the pyridine ring and Cl(2), Cl(3) atoms are coplanar (mean deviation 0.02 Å). The pendant aryl ring makes a dihedral angle of 68.9° (50.1° in **1a**) to the plane. The amide group C(5)C(6)O(1)N(2) is nearly perfectly planar.

Contraction of the metal radius upon oxidation causes a *ca.* 0.06 Å decrease in average Re–Cl distances between **1a** and **3d**. For comparison we note that between a similar phosphine oxide pair both the Re–Cl and Re–$OPPh_3$ (no back-bonding) bonds contract.[2] In contrast the Re–P length *increases* by 0.1 Å between **1a** and **3d**. This is primarily attributed to the weakening of Re–P back-bonding upon metal oxidation. The residual interaction is, however sufficient to sustain facial geometry in **3** which fails to isomerise even on prolonged boiling in toluene.

Conclusion

The *fac*-[$Re^{III}L(PPh_3)Cl_3$] **1** family having a facially configured $RePN_2Cl_3$ coordination sphere has been synthesized *via* ligand displacement from *mer*-[$Re^{III}L(OPPh_3)Cl_3$] **2**. The facial geometry of **1** is a result of the optimization of Re–PPh_3 and Re–L back-bonding. The electrochemical and chemical oxidation of **1** is stereoretentive and has furnished *fac*-[$Re^{IV}L'(PPh_3)Cl_3$] **3** in which the rhenium(IV) state is stabilized by amide bonding. The Re–P back-bonding and bond length orders are respectively **1** > **3** and **1** < **3**.

Experimental

Materials

[$ReL(OPPh_3)Cl_3$],[3] [$ReOCl_3(PPh_3)_2$][18] and pyridine-2-aldimine[19] were prepared by reported methods. The purification and drying of dichloromethane and acetonitrile for synthesis as well as for electrochemical work were done as described.[20] Toluene and benzene were distilled over sodium before use. All other chemicals and solvents were of reagent grade and used as received.

Physical measurements

Spectra were recorded with the following equipment: electronic spectra, Hitachi 330 spectrophotometer; infrared spectra (KBr disc, 4000–300 cm^{-1}), Perkin-Elmer 783 spectrophotometer, proton NMR spectra were recorded on a Bruker FT 300 MHz spectrometer. Electrochemical measurements were done by using a PAR model 370-4 electrochemistry system as described.[13b] All experiments were performed at a platinum working electrode under a dinitrogen atmosphere, the supporting electrolyte being tetraethylammonium perchlorate. The potentials are referenced to the saturated calomel electrode (SCE) and are uncorrected for the junction contribution. Magnetic susceptibilities were measured on a PAR-155 vibrating sample magnetometer. Microanalyses were done by using a Perkin-Elmer 240C elemental analyser.

Syntheses

***fac*-[$Re^{III}L(PPh_3)Cl_3$] 1.** The complexes were prepared by the same general methods. Details are given for **1b** (L = L^2).

To a pink solution of *mer*-[$ReL^2(OPPh_3)Cl_3$] (100 mg, 0.14 mmol) in dry benzene (15 cm^3), PPh_3 (200 mg, 0.75 mmol) was added and the mixture was heated to reflux under pure nitrogen for 1 h affording a violet solution which yielded crystalline *fac*-[$ReL^2(PPh_3)Cl_3$] (20 mg) upon cooling to room temperature. The complex was collected by filtration and the filtrate was stripped of solvent. The residue was dissolved in a small volume of CH_2Cl_2 and subjected to chromatography on a silica gel column prepared in benzene. Upon elution with benzene–acetonitrile (25:1, 15:1 and 10:1) *mer*-[$ReL^2(OPPh_3)Cl_3$] (18 mg), *mer*-[$ReL^2(NC_6H_4Me)Cl_3$] (7 mg) and *fac*-[$ReL^2(PPh_3)Cl_3$] (28 mg) were successively isolated. The total yield of bluish violet *fac*-[$ReL^2(PPh_3)Cl_3$] is 48 mg, 50%.

The complex was also synthesized starting from a solution of [$ReOCl_3(PPh_3)_2$] (100 mg, 0.12 mmol) in dry benzene (15 cm^3) containing L^2 (29 mg, 0.15 mmol). The mixture was heated to reflux under pure nitrogen for 1 h. The violet solution was stripped of solvent and the residue subjected to chromatography as described above. The yield of *fac*-[$ReL^2(PPh_3)Cl_3$] was 37 mg, 40% (Found: C, 48.95; H, 3.25; N, 3.70. Calc. for $C_{30}H_{25}Cl_3N_2PRe$ **1a**: C, 48.87; H, 3.39; N, 3.80. Found: C, 48.68; H, 3.51; N, 3.61. Calc. for $C_{31}H_{27}Cl_3N_2PRe$ **1b**: C, 49.56; H, 3.60; N, 3.73. Found: C, 48.40; H, 3.35; N, 3.50. Calc. for $C_{31}H_{27}Cl_3N_2OPRe$ **1c**: C, 48.52; H, 3.52; N, 3.65. Found: C, 47.00; H, 3.25; N, 3.50. Calc. for $C_{30}H_{24}Cl_4N_2PRe$ **1d**: C, 46.69; H, 3.11; N, 3.63%).

***fac*-[$Re^{IV}L'(PPh_3)Cl_3$] 3.** The same general methods were used for all the complexes. The case of **3b** (L′ = $L^{2'}$) is detailed below.

A solution of *fac*-[$Re^{III}L^2(PPh_3)Cl_3$] (20 mg, 0.027 mmol) in wet acetonitrile (20 cm^3) containing tetraethylammonium perchlorate (25 mg, 0.11 mmol) was electrolyzed exhaustively under nitrogen at 1.0 V *vs.* SCE. The bluish violet solution changed to red and finally to yellow. The coulomb count corresponded to the transfer of three electrons, equation (4)

$$fac\text{-}[Re^{III}L(PPh_3)Cl_3] \longrightarrow fac\text{-}[Re^{IV}L'(PPh_3)Cl_3] + 3H^+ + 3e^- \quad (4)$$

(observed count, 7.25; calculated count for one electron, 2.45).

The electrolyzed solution was stripped of the solvent and the residue was washed thoroughly with hot water and then dried over P_4O_{10}, yielding pure yellow *fac*-[$ReL^{2'}(PPh_3)Cl_3$]. The yield was 14 mg, 72%.

Chemical synthesis of the complex was achieved by oxidation of *fac*-[$ReL^2(PPh_3)Cl_3$] (50 mg, 0.067 mmol) in acetonitrile (20 cm^3) by aqueous HNO_3 (0.5 M, 0.5 cm^3). The mixture was stirred for 1 h at room temperature affording a yellow solution [hydrogen peroxide (0.5 cm^3, 30%) requires 12 h stirring in an ice bath]. The solvent was removed and the residue washed and dried as above, yielding *fac*-[$ReL^{2'}(PPh_3)Cl_3$]. The yield was 40 mg, 80% (Found: C, 47.80; H, 3.25; N, 3.60. Calc. for $C_{30}H_{24}Cl_3N_2OPRe$ **3a**: C, 47.89; H, 3.19; N, 3.73. Found: C, 48.80; H, 3.25; N, 3.50. Calc. for $C_{31}H_{25}Cl_3N_2OPRe$ **3b**: C, 48.58; H, 3.40; N, 3.66. Found: C, 47.50; H, 3.42; N, 3.45. Calc. for $C_{31}H_{26}Cl_3N_2O_2PRe$ **3c**: C, 47.59; H, 3.33; N, 3.58. Found: C, 46.00; H, 2.80; N, 3.65. Calc. for $C_{30}H_{23}Cl_4N_2OPRe$ **3d**: C, 45.79; H, 2.93; N, 3.56%).

Conversion of *fac*-[$Re^{III}L^2(PPh_3)Cl_3$] to *mer*-[$Re^{V}L^2(NC_6H_4Me)Cl_3$]

A solution of *fac*-[$ReL^2(PPh_3)Cl_3$] (50 mg, 0.067 mmol) in toluene (10 cm^3) was heated to reflux for 1 h in the presence of *p*-toluidine (35 mg, 0.33 mmol). The violet solution was stripped of solvent and the residue was subjected to chromatography on a silica gel column using benzene–acetonitrile (15:1) as the eluent. The complex *mer*-[$ReL^2(NC_6H_4Me)Cl_3$] was isolated (yield 35 mg, 88%) by removing the solvent.

Crystallography

Dark prismatic crystals of **1a** and orange prismatic crystals of **3d** were grown by slow diffusion of hexane into dichloromethane solutions of the respective complexes.

Cell parameters were determined by a least-squares fit of 30 machine-centered reflections (2θ = 15–30°). Data were collected by the ω-scan technique in the range $3 \leqslant 2\theta \leqslant 45°$ for **1a** and $3 \leqslant 2\theta \leqslant 47°$ for **3d** on a Siemens R3m/V four-circle diffractometer with graphite-monochromated Mo-Kα radiation (λ = 0.71073 Å). Two check reflections after every 198 showed no intensity reduction. All data were corrected for Lorentz-polarization and absorption.[21] The metal atoms were located from Patterson maps, and the rest of the non-hydrogen atoms emerged from successive Fourier syntheses. The structures were then refined by a full-matrix least-squares procedure on F^2. All non-hydrogen atoms [except O(2) for **3d**] were refined anisotropically. All hydrogen atoms were included in calculated

Table 5 Crystal data for [Re^{III} L^1(PPh$_3$)Cl$_3$] **1a** and [Re^{IV}L$^{4'}$(PPh$_3$)Cl$_3$] **3d**

Complex	**1a**	**3d**
Formula	$C_{30}H_{25}Cl_3N_2PRe$	$C_{30}H_{23}Cl_4N_2OPRe \cdot H_2O$
M	737.04	804.49
Crystal size/mm	0.5 × 0.2 × 0.15	0.42 × 0.32 × 0.2
Crystal system	Monoclinic	Triclinic
Space group (no.)	$P2_1/n$ (14)	$P\bar{1}$ (2)
a/Å	11.505(6)	9.994(6)
b/Å	13.545(5)	11.617(6)
c/Å	18.720(11)	15.135(9)
α/°	—	76.26(4)
β/°	97.66(4)	88.11(5)
γ/°	—	67.40(4)
U/Å^3	2891(3)	1573(2)
Z	4	2
D_c/g cm^{-3}	1.693	1.699
μ(Mo-Kα)/cm^{-1}	45.58	42.85
F(000)	1440	786
Transmission coefficient	0.56/1.00	0.53/1.00
Total reflections	4105	4733
Number unique reflections (R_{int})	3801 (0.03)	4663 (0.051)
Number observed reflections [$I > 2\sigma(I)$]	3065	4054
Data/restraints/parameters	3797/0/334	4652/0/357
$R1$,[a] $wR2$[b] [$I > 2\sigma(I)$]	0.0316, 0.0680	0.0506, 0.1319
$R1$, $wR2$ (all data)	0.0485, 0.0851	0.062, 0.1554
Goodness of fit on F^2	1.040	1.153
Maximum and mean Δ/σ	0.002/0.000	0.002/0.000
Maximum, minimum difference peaks/e Å^{-3}	0.672, −0.849	3.087, −1.727

[a] $R1 = \Sigma||F_o| - |F_c||/\Sigma|F_o|$. [b] $wR2 = [\Sigma w(F_o^2 - F_c^2)^2/\Sigma w(F_o^2)^2]^{\frac{1}{2}}$.

positions. The programs of SHELXTL™ V 5.03 (Bruker Analytical X-ray Systems: Part Number 269-015900) were utilized. Significant crystal data are listed in Table 5. The relatively large residual maxima in the case of **3d** occurred very close (<1 Å) to the metal/chloride sites and are assigned to ghosts caused by series-termination effects. CCDC reference number 186/1224.

See http://www.rsc.org/suppdata/dt/1999/155/ for crystallographic files in .cif format.

Acknowledgements

We thank the Department of Science and Technology, Indian National Science Academy and the Council of Scientific and Industrial Research, New Delhi for financial support. Affiliation with the Jawaharlal Nehru Centre for Advanced Scientific Research, Bangalore is acknowledged.

References

1 M. Menon, S. Choudhury, A. Pramanik, A. K. Deb, S. K. Chandra, N. Bag, S. Goswami and A. Chakravorty, *J. Chem. Soc., Chem. Commun.*, 1994, 57.

2 M. Menon, A. Pramanik, N. Bag and A. Chakravorty, *Inorg. Chem.*, 1994, **33**, 402.

3 B. K. Dirghangi, M. Menon, A. Pramanik and A. Chakravorty, *Inorg. Chem.*, 1997, **36**, 1095.

4 B. K. Dirghangi, S. Banerjee, M. Menon and A. Chakravorty, *Indian J. Chem., Sect. A*, 1997, **36**, 249.

5 S. Banerjee, B. K. Dirghangi, M. Menon, A. Pramanik and A. Chakravorty, *J. Chem. Soc., Dalton Trans.*, 1997, 2149.

6 B. K. Dirghangi, M. Menon, S. Banerjee and A. Chakravorty, *Inorg. Chem.*, 1997, **36**, 3595.

7 H. P. Gunz and G. J. Leigh, *J. Chem. Soc. A*, 1971, 2229.

8 F. Tisato, F. Refosco, C. Bolzati, A. Cagnolini, S. Gatto and G. Bandoli, *J. Chem. Soc., Dalton Trans.*, 1997, 1421.

9 J. C. Bryan, R. E. Stenkamp, T. H. Tulip and J. M. Mayer, *Inorg. Chem.*, 1987, **26**, 2283.

10 G. Rouschias and G. Wilkinson, *J. Chem. Soc. A*, 1967, 993; J. V. Caspar, B. P. Sullivan and T. J. Mayer, *Inorg. Chem.*, 1984, **23**, 2104; B. K. Dirghangi, Ph.D. Thesis, Jadavpur University, 1998.

11 A. S. M. Al-Shihri, J. R. Dilworth, S. D. Howe, J. Silver and R. M. Thompson, *Polyhedron*, 1993, **12**, 2297; X. L. R. Fontaine, E. H. Fowles, T. P. Lyzell, B. L. Shaw and M. Thornton-pett, *J. Chem. Soc., Dalton Trans.*, 1991, 1519; R. Rossi, A. Duatti and L. Magon, *J. Chem. Soc., Dalton Trans.*, 1982, 1949.

12 M. Hirsch-Kuchma, T. Nicholson, A. Davison, W. M. Davis and A. G. Jones, *J. Chem. Soc., Dalton Trans.*, 1997, 3185; M. Luaphon, P. E. Fanwick and R. A. Walton, *Inorg. Chem.*, 1990, **29**, 4348.

13 (*a*) F. A. Cotton and G. Wilkinson, *Advanced Inorganic Chemistry*, John Wiley & Sons, New York, 5th edn., 1988, p. 64; (*b*) A. Pramanik, N. Bag, D. Ray, G. K. Lahiri and A. Chakravorty, *Inorg. Chem.*, 1991, **30**, 410.

14 H. Brunner and W. A. Herrmann, *Chem. Ber.*, 1972, **105**, 770; M. N. Ackermann, C. R. Barton, C. J. Deodence, E. M. Specht, S. C. Keill, W. E. Schreiber and H. Kim, *Inorg. Chem.*, 1989, **28**, 397.

15 P. Ghosh, A. Pramanik, N. Bag and A. Chakravorty, *J. Chem. Soc., Dalton Trans.*, 1992, 1883.

16 M. Menon, A. Pramanik and A. Chakravorty, *Inorg. Chem.*, 1995, **34**, 3310.

17 H. Taube, *Electron Transfer Reactions of Complex ions in Solution*, Academic Press, New York, 1973, p. 73.

18 J. Chatt and G. A. Rowe, *J. Chem. Soc.*, 1962, 4019.

19 G. Bähr and H. Z. Thamlitz, *Z. Anorg. Allg. Chem.*, 1955, **282**, 3.

20 P. Basu, S. Bhanja Choudhury and A. Chakravorty, *Inorg. Chem.*, 1989, **28**, 2680.

21 A. C. T. North, D. C. Philips and F. S. Mathews, *Acta Crystallogr., Sect. A*, 1968, **24**, 351.

Paper 8/06346J